Chinese J. Chem. Eng., **12** (6) 831 – 835 (2004)

Ice Crystal Sizes and Their Impact on Microwave Assisted Freeze Drying

WU Hongwei(吴宏伟)[a,b], **TAO Zhi(陶治)**[b], **GAO Ping(高平)**[a] and **CHEN Guohua(陈国华)**[a,*]

[a] Department of Chemical Engineering, The Hong Kong University of Science and Technology, Clear Water Bay, Kowloon, Hong Kong, China

[b] Department of Power Engineering, The Beijing University of Aeronautics and Astronautics, Beijing 100083, China

Abstract Freeze drying of an aqueous solution would result in the non-uniform distribution of solute concentration. Because ice is almost transparent to microwave, therefore such a non-uniform distribution may affect the microwave assisted freeze drying. The direct observation of the ice crystals formed under microscope reveals that the ice crystal sizes formed from de-ionized water depend on the cooling rate with fast cooling rate giving smaller ice crystals as expected. Once there is a sufficient amount of solute mixed with the de-ionized water, for example the reactive red, the size and its distribution are not very much dependent on either cooling rate or the final temperature provided there is sufficient time of cooling and the final temperature is not too low. The size of ice crystals formed within the solution of reactive red is usually below 100 μm with a freezing rate of 1°C·min^{-1} for a droplet of the size of less than 1 mm. A simplified simulation indicates that such a small ice crystal would not cause a significant non-uniform distribution of temperature for microwave assisted freeze drying. When the ice crystal size is larger than 5 mm, heat conduction from the solute concentrated region to the ice region may need to be considered.

Keywords cooling rate, ice morphology, microscopical observation, temperature

1 INTRODUCTION

Ice crystals formation has been investigated by several researchers theoretically or experimentally[1–6]. For frozen product, the desired product characteristics, *i.e.* texture and storage stability, can be obtained by precise control of the crystalline structure[7,8]. The characteristics of the ice crystals would also affect the quality of freeze-dried food. The influence of freezing rate on the size of the ice crystal is well known qualitatively. Quick freezing results in smaller crystals and reduces the freeze concentration, but may also lead to incomplete crystallization. In contrast, slow freezing produces larger crystals and allows higher sublimation speed[9]. As it is known that freeze drying is a time consuming process due to the limited heat supply from either the dried layer by radiation and conduction or from the frozen layer by conduction only. Recently, microwave assisted drying has attracted significant attention because of its unique feature of volumetric heating that can significantly reduce the drying time[10–14].

For microwave assisted freeze-drying, the enhanced drying rate was also reported[15]. Because ice is almost transparent to microwave heating, the energy absorbed by the frozen product has to be transferred from the solid matrix to ice crystal surface where sublimation may take place. In the case of producing powder from freeze-drying such as freeze-dried coffee or pharmaceutical products, the freezing condition is expected to affect the distribution of solids within the frozen product. This inevitable fact may affect the quality of freeze-drying not only through the size of crystals but also through the mal-distribution of temperatures within the product under drying. Such an analysis has not been found in literature. Hence it becomes the objective of the present study. In this paper, we show the results of ice crystal size and solute distributions by observing the frozen sample under a microscope. Different freezing conditions were tested. Reactive red dye was used in order to have a clear image of the samples.

2 EXPERIMENTAL SETUP

The schematic diagram of the cooling system is shown in Fig. 1. The LNP cooling system can be used to cool a sample down to below −194℃. The continuous supply of liquid nitrogen was provided by employing a large capacity cylinder. The two litre desktop dewar flask with the fitted pipe (D2L) was used when a fast cooling rate was desired. The device works by drawing liquid nitrogen from the flask through a very small bore tube *via* a filter, so as to prevent the blockage from ice particles, then the nitrogen gas is vaporized and passed into a valve allowing manual control of the flow rate. A small quantity of gas was also drawn through the window gas tube to prevent condensation on the top surface of the lid window.

A droplet of the sample to freeze was supplied from

Received 2002-10-25, accepted 2003-01-20.

* To whom correspondence should be addressed. E-mail: kechengh@ust.hk

a syringe. It was placed on the glass cover. The inside of the metal vessel was purged before the introduction of the sample. The droplet was cooled from room temperature (about 23 ℃) to final temperature (−40℃) at desired cooling rates. The samples were observed directly through the window attached to the vessel with the help of an Olympus Microscope BX50 (Olympus Optical Co., Japan). A high resolution optical camera recorded the images for analysis.

3 RESULTS AND DISCUSSION

3.1 Typical crystal morphology in de-ionized water

Fig. 2(a)—Fig. 2(c) show the typical morphologies of ice crystals formed from de-ionized water at a cooling rate of 1 ℃·min^{-1}. It is obvious that the center of the droplet does not give a clear picture of the crystal geometries. The small bean like particles on top of the bulk may be the result of the concentrated impurities. The large scale shade differences of the image may reflect the roughness of the surface rather than the crystal sizes because there are not solute added in the de-ionized water. It is interesting but not essential for drying to observe that there are always some clusters of crystals formed away from the main droplet. That is, the freezing of the droplet tends to contract from its original size because the glass surface is hydrophilic. Because of the interfacial interaction between water and glass, some water cannot move with the surface contraction rate. Hence the formation of orphaned ice crystals was observed. Obviously, the size of this type of ice crystals depends on the cooling rate and also

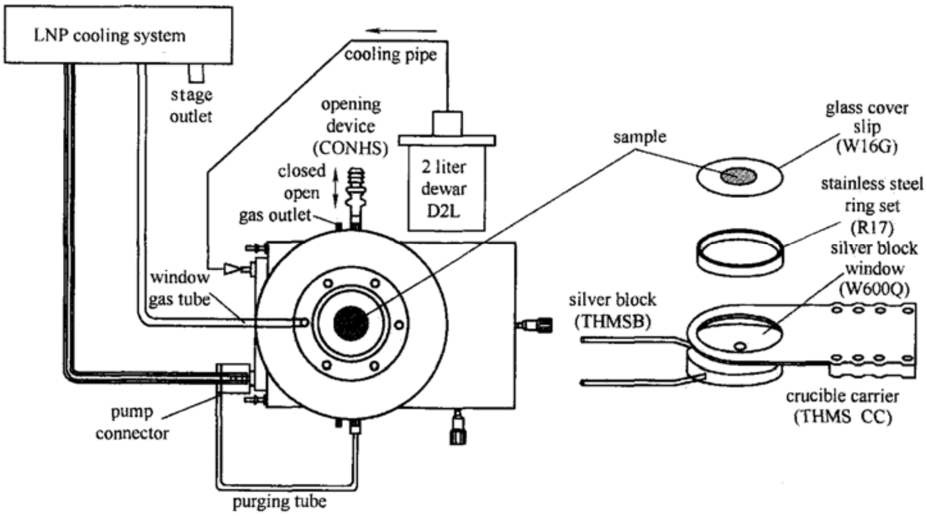

Figure 1 Schematic diagram of the cooling and imaging system

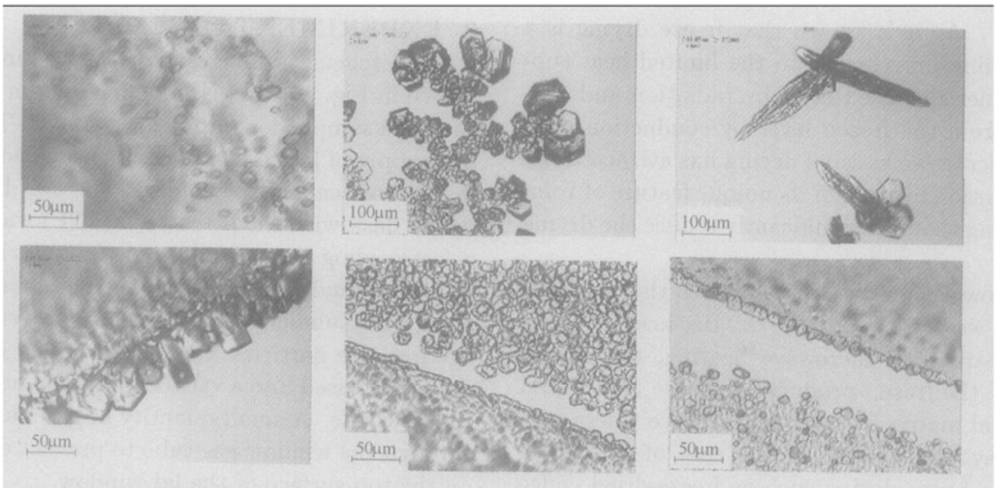

Figure 2 Morphology changes of the ice crystals formed from cooling de-ionized water
(cooling rate: 1℃·min^{-1}, end temperature: −40℃)
(a) upper left—image at center; (b) upper-middle—image outside the bulk; (c) upper-right—image of individual ice crystals;
(d) lower-left—image at the edge; (e) lower-middle—image at the edge with cooling rate of 3℃·min^{-1};
(f) lower-right—image at the edge with cooling rate of 5℃·min^{-1}

the property of the glass surface. It has a wide range of distribution, Fig. 2(b). It may be of help to see that the shape of the crystals found outside the main ice can be of the image as shown in Fig. 2(c). The ice crystals were formed without the presence of air. The image of the edge of the droplet, Fig. 2(d), may show some insight of the crystal sizes. It can be seen that most of the crystals there have a size below 50 μm at a cooling rate of 1 °C·min^{-1}. An increase in cooling rate results in the formation of small crystals as shown in Figs. 2(d)—(f).

3.2 Ice crystals formed from solution of reactive red HE-3B

When some solids are mixed with the de-ionized water, the ice growing history becomes very different as seen from Fig. 3. The six images were taken along with the decrease of the freezing temperature with about four minutes apart from adjacent pictures except the last one which was taken after holding the frozen sample for 10 min at −40℃. The growth of the ice crystal size is clearly observed. Compared with the picture seen in Fig. 2(d)—(f), the sizes of the crystals are much smaller for the solution with reactive red HE-3B introduced. This is reasonable because the solute in the solution provides more nuclei for ice crystals to grow. The similar shapes between Fig. 3(c) and (d) show that when the temperature reached −35℃, the freezing of the sample was almost completed. Holding the ice at a low temperature for a short while does not change the shape of the crystals formed.

With the introduction of reactive red, it is now possible to observe the ice crystals in the center of the frozen droplet as shown in Fig. 4 where the effects of freezing rate and final temperature were displayed. It can be seen clearly that the solute was pushed toward and concentrated at the conjunction surfaces of adjacent ice crystals. This results in a non-uniform distribution of the solute within the frozen droplet. The cooling rate gives only minor effect on the size of the crystals. The final cooling temperature does not show significant influence either except one condition with the largest cooling rate and the lowest cooling temperature. The similarities among Fig. 4 (a1)—(c3) may be explained by the fact that −30℃ is probably sufficient cold for the freezing of the solution even at the rate of 5℃·min^{-1}. The smaller size of the ice crystals shown in Fig. 4 (c4) demonstrates that when the freezing rate is 10℃·min^{-1}, one only has slightly longer than 2 min to cool the sample to the freezing point. The rate of heat transfer may limit the formation of ice at a temperature higher than −70℃. In other words, the formed ice crystals may be obtained at a temperature other than that indicated by the temperature measured inside the cooling chamber. Anyhow, it is seen that fast cooling with low final temperature gives a more uniform solute concentration distribution with typical ice crystal size being 50 μm. For the mild cooling conditions, the size of the ice crystals is seldom larger than 100 μm. Even if the solute concentration is reduced to a quarter of that shown in Fig. 4, the ice crystal sizes are not very much different as seen in Fig. 5. The only difference is that the amount of solute at the edges of adjacent crystals is smaller for the low concentration solution. The results shown in Figs. 4 & 5 imply that the size of the ice crystals do not depend on the number of nuclei once there are sufficient amount exists.

3.3 Implication of the non-uniform solute distribution on MW freeze-drying

As discussed in the introduction section, the non-

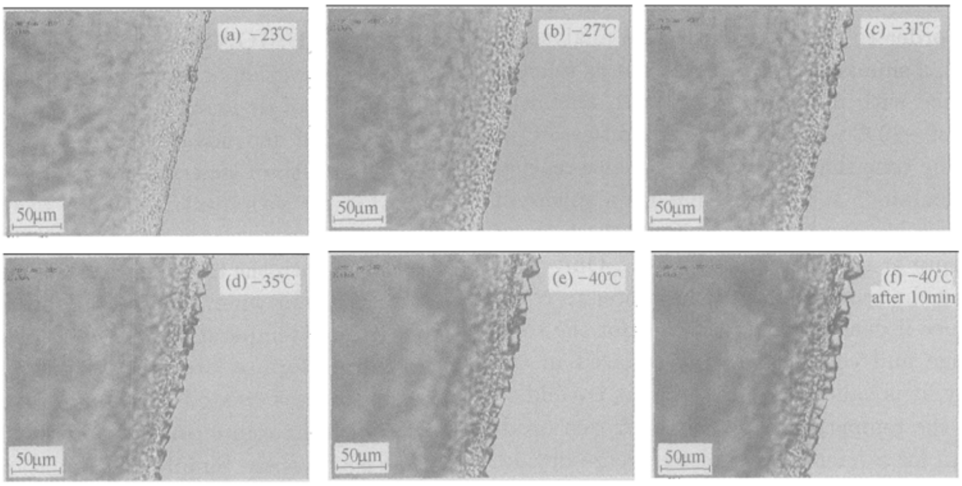

Figure 3 **The growth of ice crystals in 1.0 g·L^{-1} reactive red HE-3B aqueous solution**
[the sample was frozen at −22.3℃ at a cooling rate of 1℃·min^{-1} and end temperature of −40℃. the temperatures inside the images indicate the value when the picture was taken except for (f)]

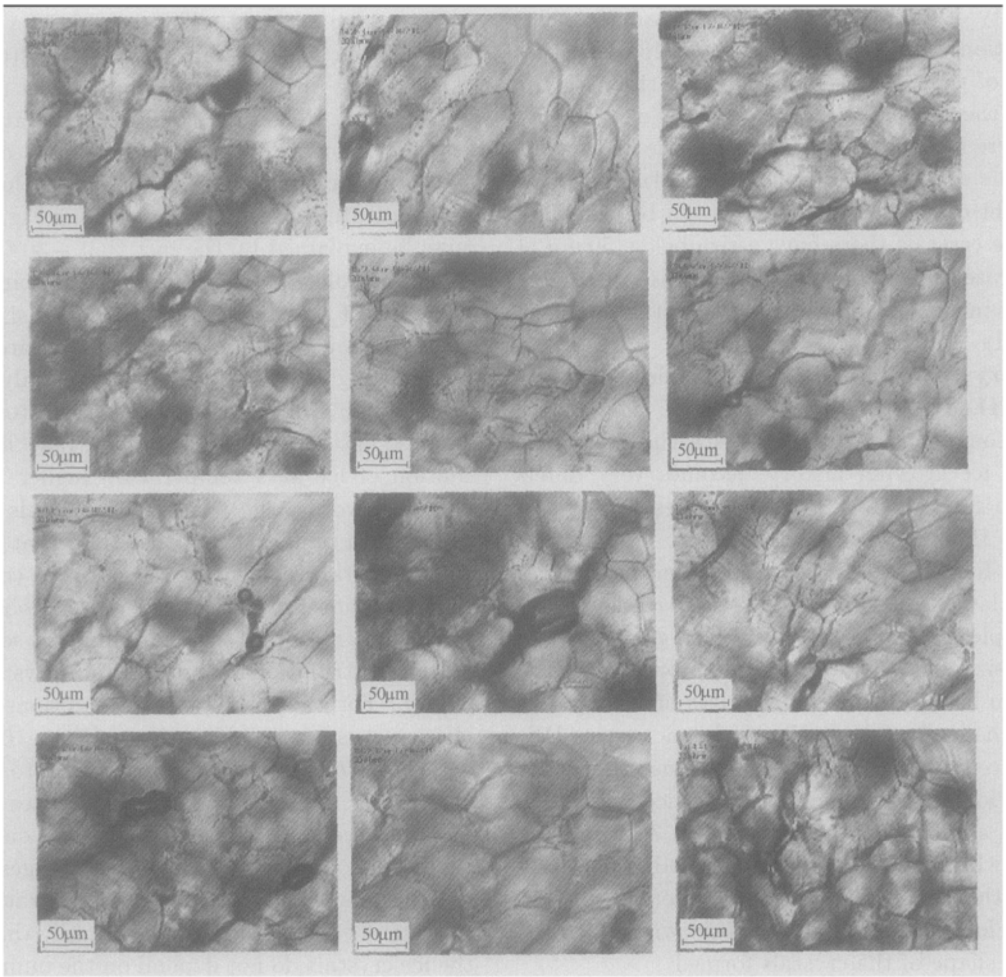

Figure 4 **The change of ice crystals in 1.6 g·L^{-1} reactive red HE-3B aqueous solution**
end temperature, ℃: (a) left column −30; (b) middle column −50; (c) right column −70
cooling rate, ℃·min^{-1}: (1) first row 1; (2) second row 3; (3) third row 5; (4) forth row 10

uniform distribution of the solute in the frozen product will affect the adsorption of microwave energy and also the temperature distribution within the frozen material. In order to have a quantitative analysis of such an effect, a simulation was carried out as follows. A sphere of ice with different radius with an initial temperature of −20℃ was suddenly heated to −5℃ at its surface. The time that the center of the ice reaches −6℃ was calculated. It is noted that for a sphere of 100 μm in diameter, it requires only 0.0005 s to have the temperature at the center reach −6℃. Only 1 ms is required for the temperature at the center to reach −5.05℃. Hence it can be concluded that for the temperature range and cooling rate investigated in the present study, it is valid to assume that it is valid to assume that the temperature within the frozen product is uniform for a microwave assisted freeze drying. If the ice crystal is large, say larger than 5 mm in diameter, the heat conduction from the solute concentrated region to the ice region may be considered in order to have a meaningful understanding of the microwave assisted freeze drying.

4 CONCLUSIONS

The observation of the images obtained from freezing droplets of de-ionized water reveals that the size of ice crystals depends on the freezing rate. The progressive growth of ice crystals within a solution of deionized water with reactive red dye was recorded. The size of the ice crystals within the solution do not vary very much with the freezing rate or final freezing temperature except when the freezing rate is 10 °C·min^{-1} and the end temperature is −70℃. The sizes of the ice crystals formed are mostly under 100 μm. The freezing process created a non-uniform distribution of solute with the solute concentrated at the edges of adjacent ice crystals. Simplified simulation results show that such a non-uniform distribution does not cause a significant non-uniform distribution of temperature for the conditions investigated in the present study.

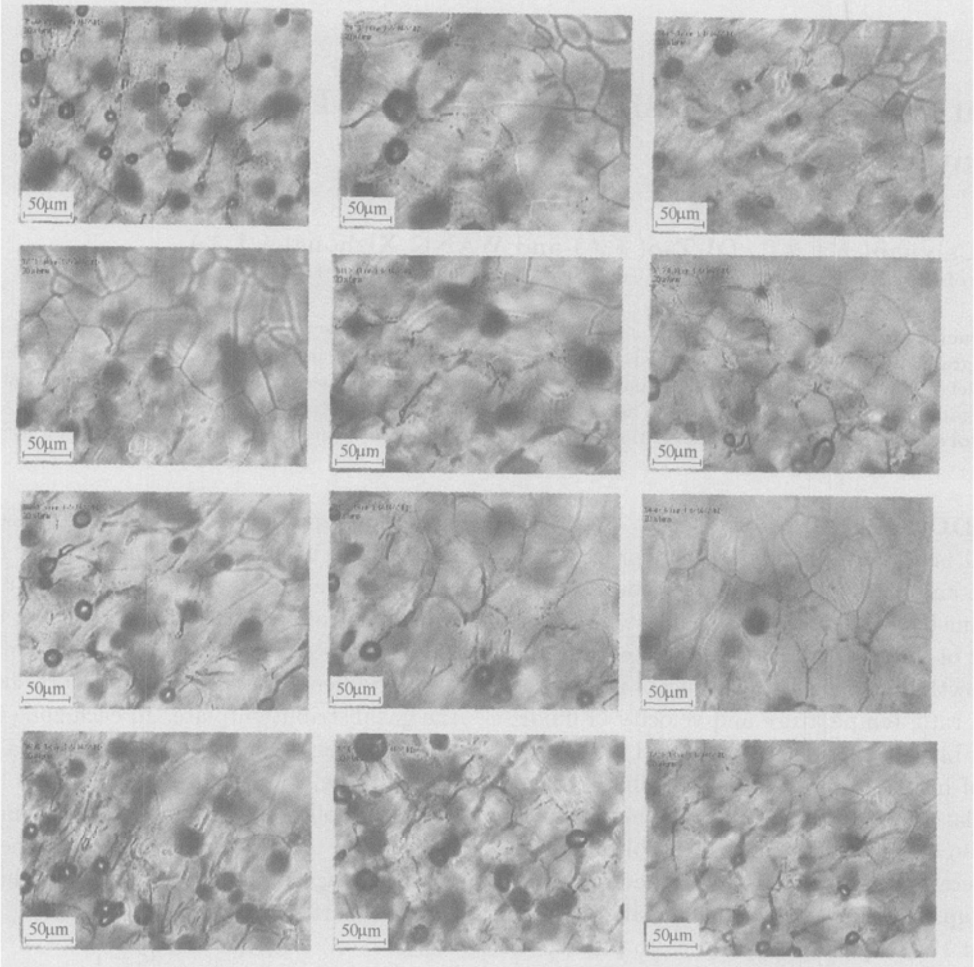

Figure 5 **The change of ice crystals in $0.4\,\mathrm{g{\cdot}L^{-1}}$ reactive red HE-3B aqueous solution**
end temperature, ℃: (a) left column −30; (b) middle column −50; (c) right column −70
cooling rate, $℃{\cdot}\mathrm{min}^{-1}$: (1) first row 1; (2) second row 3; (3) third row 5; (4) forth row 10

Only when the ice crystals are larger than 5 mm in diameter then the heat conduction from the solute to the ice has to be considered.

REFERENCES

1 Hallet, J., "Nucleation and growth of the ice crystals", In: Advances in Freeze-Drying, Herman-Verlag, Paris 21—38 (1966).

2 Nada, H., Furukawa, Y., "Anisotropic growth kinetics of ice crystals from water studied by molecular dynamics simulation", *Journal of Crystal Growth*, **169**, 587—597 (1996).

3 Shichiri, T., "Faceted ice crystals grown in water without air", *Journal of Crystal Growth*, **187**, 133—137 (1998).

4 Suzuki, Y., Takeda, T., Inazu, K., Sakamoto, T., "Freeze-drying of cephalothin sodium-granularly agglomerated crystallization during freezing.1", *Bio. Pharm. Bull.*, **16** (4), 402—406 (1993).

5 Suzuki, Y., Takeda, T., Inazu, K., Sakamoto, T., "Freeze-drying of cephalothin sodium-granularly agglomerated crystallization during freezing.2", *Bio. Pharm. Bull.*, **16** (4), 407—413 (1993).

6 Tan, C.S., Vlug, I.J.A., Stalpers, J.A., van Ingen, C.W., "Microscopical observations on the influence of the cooling rate during freeze-drying of conidia", *Mycologia*, **86** (2), 281—289 (1994).

7 Bald, W.B., Food Freezing: Today and Tomorrow, Springer-Verlag, New York, 146 (1991).

8 Hartel, R.W., Crystallization in Foods, Aspen Publishers, Gaithersburg, 1—9 (2001).

9 Rey, L., May, J.C., Freeze-Drying/Lyophilization of Pharmaceutical and Biological Products, Marcel Dekker, New York 87, (1999).

10 Constant, T., Moyne, C., Perre, P., "Drying with internal heat generation: theoretical aspects and application to microwave heating", *AIChE J.*, **42** (2), 359—368 (1996).

11 Doelling, M.K., Nash, R.A., "The development of a microwvae fuidized-bed processor. II. Drying performance and physical characteristics of typical pharmaceutical granulations", *Pharm. Res.*, **9**, 1493—1501 (1992).

12 Doelling, M.K., Jones, D.M., Smith, R.A., Nash, R.A., "The development of a microwvae fuidized-bed processor. I. Construction and qualification of a prototype laboratory unit", *Pharm. Res.*, **9**, 1487—1492 (1992).

13 Kudra, T., "Dielectric drying of particulate materials in a fluidized state", *Drying Technology*, **7** (1), 17—34 (1989).

14 Chen, G., Wang, W., Mujumdar, A.S., "Theoretical study of microwave heating patterns on batch fluidized bed drying of porous material", *Chemical Engineering Sciences*, **56** (24) 6823—6835 (2001).

15 Lombrana, J.I., Zuaso, I., Ikara, J., "Moisture diffusivity behavior during freeze drying under microwave heating power application", *Drying Technology*, **19** (8), 1613—1627 (2001).